Quantum versus Classical Annealing: Insights from Scaling Theory and Results for Spin Glasses on 3-Regular Graphs

Cheng-Wei Liu, Anatoli Polkovnikov, and Anders W. Sandvik

Quantum versus classical annealing—insights from scaling theory and results for spin glasses on 3-regular graphs

Cheng-Wei Liu, Anatoli Polkovnikov, and Anders W. Sandvik

Department of Physics, Boston University, 590 Commonwealth Avenue, Boston, Massachusetts 02215, USA

(Dated: February 23, 2015)

We discuss an Ising spin glass where each $S = 1/2$ spin is coupled antiferromagnetically to three other spins (3-regular graphs). Inducing quantum fluctuations by a time-dependent transverse field, we use out-of-equilibrium quantum Monte Carlo simulations to study dynamic scaling at the quantum glass transition. Comparing the dynamic exponent and other critical exponents with those of the classical (temperature-driven) transition, we conclude that quantum annealing is less efficient than classical simulated annealing in bringing the system into the glass phase. Quantum computing based on the quantum annealing paradigm is therefore inferior to classical simulated annealing for this class of problems. We also comment on previous simulations where a parameter is changed with the simulation time, which is very different from the true Hamiltonian dynamics simulated here.

Simulated annealing (SA), which was first proposed in the context of spin glasses [1], is one of the most versatile optimization methods [2, 3]. The basic idea of SA is that a Monte Carlo (MC) simulation with slowly decreasing temperature can explore the energy (cost-function) landscape of a complex system without getting trapped in local minimums if the process is sufficiently slow (in analogy with removal of crystal defects by heating and annealing). It is natural to ponder the feasibility of similar schemes based on slow reduction of quantum fluctuations in *quantum annealing* (QA) processes. Such schemes have been explored for some time, theoretically [4–6] as well as in experiments on frustrated Ising systems such as $LiHo_xY_{1-x}F_4$ [7, 8]. The QA ideas have risen to particular prominence in the context of quantum computation [9–11], where there are now serious efforts to implement QA (also called the quantum-adiabatic algorithm) in actual devices [12], currently with ≈ 500 q-bits in the D-Wave device [13]. It is not yet clear whether true QA has been realized in these systems, however [14, 15]. Beyond this practical issue, a fundamental question is whether QA really is more efficient than SA for important optimization problems. This question has been addressed [16, 17] but so far there are few solid conclusions.

We here present a generic way to compare SA and QA, using scaling theory in combination with a quantum MC (QMC) algorithm to simulate systems out of equilibrium with Hamiltonian dynamics in imaginary time [18, 19]. We also show that this is very different from the dynamics arising when a parameter is changed versus QMC simulation time, as done in recent attempts to model a QA device [14, 15]. We present results for an essential model studied in the context of QA; a quantum $S = 1/2$ spin model on random 3-regular graphs in which all spins interact antiferromagnetically with three other spins. The corresponding classical Ising glass has an exactly known transition temperature and critical exponents [20, 21]. The quantum model includes a transverse field and has

a ground-state glass transition. Recent work has shown evidence for a continuous transition but the results were not completely conclusive [22]. Here we demonstrate a continuous transition by scaling QMC data as a function of the velocity in the imaginary-time QA scheme. The exponents governing the critical growth of glass domains show that the QA is less efficient than the corresponding SA protocol. Thus, for a large system, a quantum computer based on the QA would not pass through the glass transition faster than a classical SA process.

Quantum annealing.—Many optimization problems can be cast in the form of energy minimization of a classical Ising spin system described by a Hamiltonian

$$H_0 = \sum_{i=1}^{N} \sum_{j=1}^{N} J_{ij} \sigma_i^z \sigma_j^z, \qquad (\sigma_i^z = \pm 1). \qquad (1)$$

Challenging problems correspond to disordered frustrated interactions J_{ij}. In QA, quantum fluctuations of some form are added, e.g., a uniform transverse field

$$H_1 = h \sum_{i=1}^{N} \sigma_i^x = h \sum_{i=1}^{N} (\sigma_i^+ + \sigma_i^-). \qquad (2)$$

The total Hamiltonian is expressed as

$$H = sH_0 + (1-s)H_1, \qquad (3)$$

where $s \in [0, 1]$ regulates the quantum fluctuations. The "driver" H_1 can be chosen such that its ground state is trivial; with Eq. (2) it is the product state $|\Psi_0(0)\rangle = \prod_i |\uparrow_i + \downarrow_i\rangle$. By the adiabatic theorem [23, 24], if the change of s from 0 to 1 is sufficiently slow, the system will stay in the ground state $|\Psi_0(s)\rangle$ and in the limit $s \to 1$ one obtains an optimal solution (out of typically a large number of degenerate ones) of the classical problem.

The critical issue is how slowly s must change for the solution not to be ruined by excitations. In the 2-level Landau-Zener problem the time is $\propto \Delta^{-2}$, where Δ is

the minimum gap between the two states. Generalizing this to a many-body system with N degrees of freedom, such as Eq. (3), a quantum phase transition is expected at some point $s_c \in [0,1]$ where the ground state changes from trivial, in some sense, to complex. If at s_c the gap is Δ_N and if s is changed linearly, the required annealing time grows with N as Δ_N^{-p} [25] (though the claim $p \geq 2$ is inaccurate, as we will discuss below). Then, if $\Delta_N \to 0$ as a power of $1/N$ (in a continuous quantum phase transition) one can solve the problem using QA in polynomial time in N. For an exponentially vanishing gap (first-order transition) the time grows exponentially.

Arguments such as these have stimulated interest in numerically investigating quantum phase transitions in important quantum information problems. Initial results for one class of problems indicated a continuous transition [9, 10], but once results for larger systems became available a first-order transition seemed more likely [26, 27]. Other problems have been investigated recently [22] and some of them likely have continuous transitions.

An important issue was neglected above: The nature of the quantum state and excitations once the critical point has been passed. While in models based on Eqs. (1) and (2) the lowest excitations are gapped for $s < s_c$, the glassy state for $s > s_c$ should in general have dense gapless excitations. Therefore, going through the critical point is only the first stage of difficulties, and advancing further on the way to $s = 1$ may be exponentially hard even for a power-law closing of the gap at s_c [22]. Nevertheless, the initial passage through the transition is clearly an important step to understand and quantify. Here we obtain insights and quantitative results based on scaling properties of the quantum and classical glass transitions in antiferromagnets on 3-regular graphs.

Non-equilibrium QMC.—One reason for the currently rather poor general understanding of the efficiency of QA schemes is the difficulties of studying dynamics of large quantum many-body systems on classical computers. Recently QMC simulations realizing Schrödinger evolution in imaginary time were proposed as a way to obtain limited but valuable information [18, 19, 28]. Here we use the *quasi-adiabatic QMC* (QAQMC) method [19], where $|\Psi_0(s=0)\rangle$ is acted upon by a product of m evolving Hamiltonians $P_{m,1} = H(s_m) \cdots H(s_2)H(s_1)$, where in the simplest (linear quench) case $s_j = j\delta_s$ with $\delta_s = s_m/m$. The normalization $\langle\Psi_0(0)|P_{1,m}P_{m,1}|\Psi_0(0)\rangle$ is written as a sum over all possible strings of the operators in the terms (1) and (2), and "asymmetric expectation values" of the form

$$\langle A\rangle_\tau = \frac{\langle\Psi_0(0)|P_{1,m}P_{m,\tau+1}AP_{\tau,1}|\Psi_0(0)}{\langle\Psi_0(0)|P_{1,m}P_{m,1}|\Psi_0(0)\rangle}, \quad (4)$$

are MC evaluated. The quantity $\langle A\rangle_\tau$ approaches the ground state expectation value $\langle A(s_\tau)\rangle$ when $m \to \infty$ and for finite m it contains the same leading finite-velocity correction as in imaginary-time Schrödinger dynamics with an evolving Hamiltonian $H[s(t)]$, with $s = s_c - v(t_f - t)$, $t \in [t_i, t_f]$, and the velocity $v = ds(t)/dt = aN\delta_s$. Here the factor a is known [19] but is irrelevant for scaling, and we here use $a = 1$. Since imaginary- and real-time quenches to critical points share the same dynamic exponent z [18], real-time critical scaling behavior can be extracted using QAQMC. We can also continue past s_c into the glass phase but here our main aim is to study the dynamic criticality upon approaching s_c.

The implementation of the QAQMC method for the 3-regular graphs is a straight-forward generalization of the method developed for the standard transverse-field Ising model (TFIM) in Ref. 19. The classical part of the Hamiltonian is Eq. (1), with any given spin i coupled to exactly three other spins j, and for these pairs $J_{ij} = 1$ (antiferromagnetic). The random graphs were generated using the Steger-Wormald algorithm [29].

The physical quantity of main interest is the Edwards-Anderson spin-glass order parameter q, which is defined using two replicas (independent simulations), 1 and 2, of a given disorder realization of the random couplings;

$$q = \frac{1}{N}\sum_{i=1}^N \sigma_i^z(1)\sigma_i^z(2). \quad (5)$$

We will analyze $\langle q^2\rangle$ averaged over thousands of quenches of systems with different random couplings. As an illustration of dynamic scaling and different types of dynamics we will also study a ferromagnet, $J_{ij} = -1$ for all nearest-neighbor pairs ($j = i+1$) on a periodic chain. In this case we calculate the standard magnetization $m_z = (1/N)\sum_i \sigma_i^z$ and analyze $\langle m_z^2\rangle$.

Dynamic scaling.—We will analyze data from QAQMC simulations within the framework of the Kibble-Zurek (KZ) scaling ansatz [30, 31] and its later generalizations [32–38]. The key point here is that there is a velocity v_{KZ} separating adiabatic and non-adiabatic evolution, and for a system of length L this is given by

$$v_{KZ} \propto L^{-(zr+1/\nu)} \propto N^{-(z'r+1/\nu')}, \quad (6)$$

where ν is the equilibrium exponent governing the divergence of the correlation length, z is the dynamic exponent, and we have also introduced exponents normalized by the dimensionality d; $N = L^d$, $\nu' = \nu d$ and $z' = z/d$. The 3-regular graphs have $d = \infty$ and we will use N for the size. To convert to unprimed exponents the upper critical dimension should then be used; $d = d_u$.

The existence of a characteristic velocity suggests a generalized finite-size scaling form for singular quantities at the critical point. For quantities calculated at the final time t_f when $s = s_c$, and when $v \propto v_{KZ}$ or lower, the order parameter takes the form

$$\langle q^2\rangle \sim N^{-2\beta/\nu'}f(vN^{z'r+1/\nu'}), \quad (7)$$

and we can extract the important exponent combinations β/ν' and $z' + 1/\nu'$ using a data-collapse technique with

results for different N and v [38]. In all cases discussed below, the resulting exponents are stable and insensitive to details of the fitting procedures. We also note that the scaling form should work only at a continuous transition and its applicability, thus, supports such a transition.

Hamiltonian versus simulation dynamics.—Before presenting QAQMC results for the 3-regular graphs, let us comment on the method of changing H as a function of the simulation time (instead of the imaginary-time evolution that we advocate). This approach is normally considered with thermal QMC simulations [17, 39] but can also be implemented for QAQMC. To illustrate this we use the ferromagnetic $d = 1$ TFIM. We use a relatively large number of operators in the operator sequence in (4), $m = 4N^2$ (sufficient for ground-state convergence at all s in equilibrium), and keep s the same for all operators. The simulation starts at $s = 0$ and s is changed linearly at velocity v until $s_c = 1/2$ is reached. At this stage the magnetization is calculated. The procedure is repeated many times to obtain $\langle m_z^2 \rangle$. The velocity is defined using a time unit of a sweep of either local updates (a Metropolis procedure where small segments of spins are flipped) or cluster updates (a generalization of the Swendsen-Wang, SW, cluster updates [40, 41]) throughout the system. Using the scaling ansatz (7) for $\langle m_z^2 \rangle$, we extract the dynamic exponent characterizing the approach to the critical point with the local and cluster updates, and compare with the exponent computed with QAQMC with s is evolving within the operator string in Eq. (4). In the latter case there is no dependence on the type of MC updates (but cluster updates give results with smaller statistical errors for a given simulation time) and we should detect Hamiltonian dynamics with $z = 1$.

The scaling analysis for all the cases is presented in Fig. 1. The static exponents are those of the $d = 2$ classical Ising model, $\beta = 1/8$ and $\nu = 1$, and we use these to produce scaling plots according to the form (7). We suspect that the simulation-time dynamics should be the same as in the classical $d = 2$ Ising model with local and SW updates, and therefore test scaling with $z = 2.17$ and $z = 0.30$, respectively (as recently computed using KZ scaling in Ref. 38). The data collapse is very good in all cases for sufficiently large systems and low velocities. The lines in the log-log plots have slopes given by

$$x = \frac{d - 2\beta/\nu}{zr + 1/\nu} = \frac{1 - 2\beta/\nu'}{z'r + 1/\nu'}, \qquad (8)$$

for $v_{KZ} \lesssim v \ll 1$ [38]. For $v \approx v_{KZ}$ there is a cross-over to equilibrium finite-size scaling, where $\langle m_z^2 \rangle \propto N^{-2\beta/\nu}$. For v of order 1 there is high-velocity cross-over (not clearly seen in Fig. 1) into a size-independent $\langle m_z^2 \rangle$, governed by another scaling form [38].

The above results for the dynamic exponents obtained under different evolution schemes confirm that evolving a model in simulation time does not access Hamiltonian dynamics and has little relevance for studying QA. While
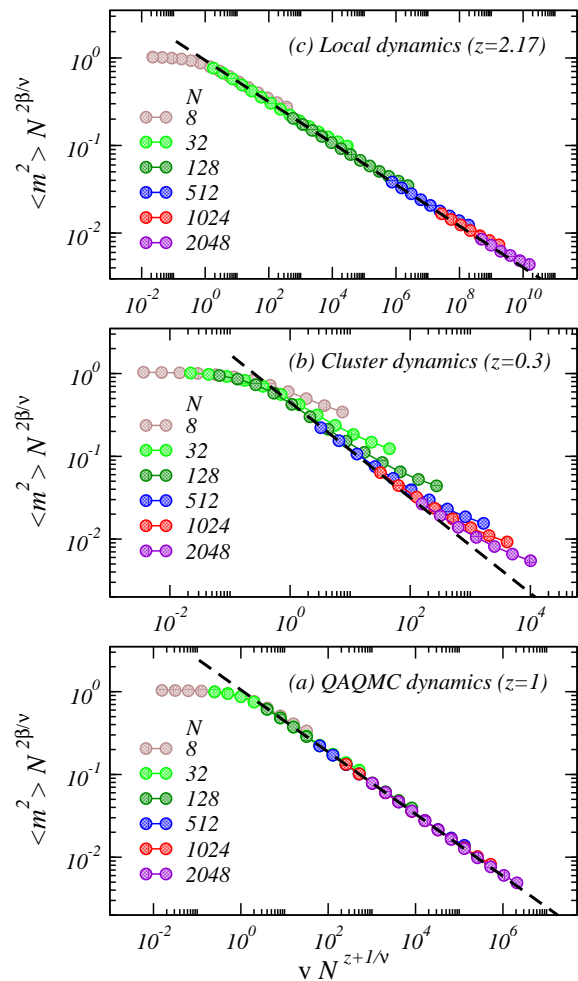

FIG. 1: (Color online) Velocity scaling for linear quenches of the TFIM: (a) Quantum quench with QAQMC Hamiltonian dynamics in imaginary time, (b) simulation-time quenches with Metropolis dynamics, and (c) SW cluster dynamics. The observed deviations from the common scaling functions are expected at an N-dependent high velocity [38].

we have here explicitly demonstrated this in the case of dynamic critical scaling, there is also no reason to expect the stochastic simulation-time dynamics to be relevant to quantum evolution in the glass phase. Hence the conclusions on the quantum mechanical nature of the dynamics of the D-Wave device drawn in Ref. 14 on the basis of such calculations are questionable (see also Ref. [15]).

QA on 3-regular graphs.—For the classical antiferromagnetic 3-regular graphs $T_c = -2 \ln^{-1}[1 - 2/(1 + \sqrt{2})]$ and the exponents, including z for SA with local updates, are also known; $\beta = 1$, $\nu' = 3$, $z' = 2/3$ ($d_u = 6$) [20, 21]. We have tested the scaling approach on this system and reproduced T_c and the exponents to within a few percent [42]. Adding the transverse field (2), based on the quantum cavity method a value $s_c \approx 0.37$ was found in Ref. 22, and QMC calculations of excitation gaps were in good agreement with this estimate. The expected errors in these calculations are of order several percent.
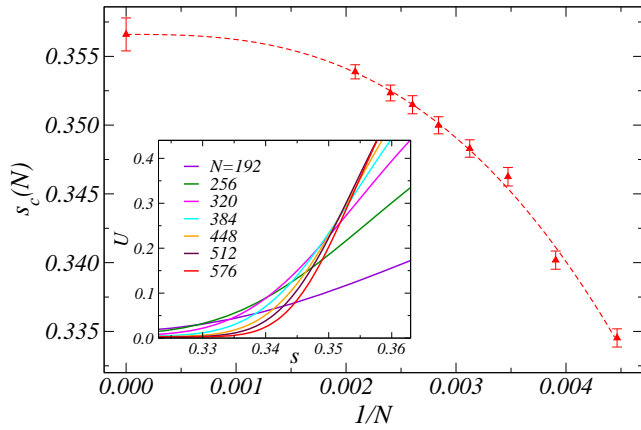
FIG. 2: (Color online) Crossing points between Binder cumulants for 3-regular graphs with N and $N+64$ spins, extracted using the curves shown in the inset. The results were obtained in quenches with $v \sim N^{-\alpha}$ for $\alpha = 17/12$. The curve in the main panel is a power-law fit for extrapolating s_c.
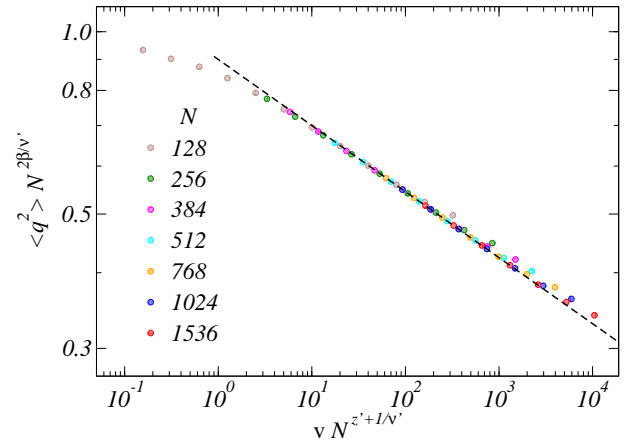

FIG. 3: (Color online) Optimized scaling collapse of the order parameter in critical quenches of 3-regular graphs, giving the exponents listed in the text. The line has slope given in Eq. (8) and the points above it (which are excluded in the fitting procedure) deviate due to high-velocity cross-overs [38].

We have located s_c using QAQMC with $v \propto N^{-\alpha}$, where α exceeds the KZ exponent $z' + 1/\nu'$ (which is unknown but later computable for *a posteriori* verification). Then $\langle q^2 \rangle \sim N^{-2\beta/\nu'}$ at s_c because $f(x)$ in Eq. (7) approaches a constant when $x \to 0$. As illustrated in Fig. 2, quenching past the estimated s_c, we use a curve crossing analysis of the Binder cumulant, $U = (3 - \langle q^4 \rangle / \langle q^2 \rangle^2)/2$, and obtain $s_c = 0.3565(12)$. This value agrees well with the previous results but has smaller uncertainty.

Performing additional quenches to the above determined s_c, we next extract critical exponents. A scaling graph with data for several system sizes is shown in Fig. 3. Here the exponents are treated as adjustable parameters for obtaining optimal data collapse. After performing an error propagation analysis we obtain $\beta/\nu' = 0.43 \pm 0.02$ and the KZ exponent $z' + 1/\nu' = 1.34 \pm 0.11$.

Interestingly, the exponents, in particular the KZ exponent, differ from those obtained using Landau theory [43] and other methods [44] for large-d and fully connected ($d = \infty$ [45]) Ising models in a transverse field; $\beta = 1$, $\nu' = 2$ and $z' = 1/4$ ($d_u = 8$), i.e., $\beta/\nu' = 1/2$ and $z' + 1/\nu' = 3/4$. In the simplest scenario the 3-regular graphs should have the same exponents. However, a QMC calculation for the fully-connected model in Ref. 46 was also not in complete agreement with the above values. It was argued that $z = 4$ ($z' = 1/2$ if $d_u = 8$), $\nu = 1/4$ ($\nu' = 2$), and $\beta \approx 1$, thus $\beta/\nu' \approx 0.5$ and $z' + 1/\nu' = 1$. We have also studied this system using the same methods as discussed above and obtained $z' + 1/\nu' = 1.33 \pm 0.12$ and $\beta/\nu' = 0.47 \pm 0.03$, in good agreement with the values for the 3-regular graphs (and s_c agrees well with Ref. 46). One potential source of disagreement with the large-d analytical calculations is the presence of logarithmic scaling corrections, not only at d_u but also at $d = \infty$, as mentioned in Ref. 43. However, we do not see any obvious signs of log corrections and

the discrepancy in $z' + 1/\nu'$ appears larger than might be expected from logs alone. Our results therefore suggest other, unknown effects in the quantum spin glass.

Implications for quantum computing.—In the classical case the KZ exponent is $z' + 1/\nu' = 1$, while in the quantum system $z' + 1/\nu' \approx 1.3$. Thus, by Eq. (6) the adiabatic annealing time grows *faster* with N in QA. Furthermore, since the order parameter scales as $N^{-\beta/\nu'}$, the critical cluster is less dense with QA, i.e., further from the solution at $s = 1$. Thus, in both these respects QA in the problem considered here performs worse than SA in passing through the critical boundary into the extended glass phase in the (h, T) plane. While our results do not contain any quantitative information on the process continuing from s_c to $s = 1$ (where the annealing time may grow exponentially in N [22]), it is discouraging that the important initial stage of QA in reaching the glass phase is less efficient than SA. It is known that QA can, in principle, be made more efficient than SA for a given problem by changing the quantum term (the driver) [47, 48]. However, to make fair comparisons, one should then allow also more complex SA evolution, e.g., going beyond just changing T.

It would be interesting to study velocity scaling also with the D-Wave device [12, 13], not only with complex frustrated couplings but even in simpler cases such as a critical ferromagnet. This would give valuable insights into the annealing process, which in the D-wave device certainly is influenced by temperature effects [12], in contrast to $T = 0$ coherent quantum dynamics studied here.

[1] S. Kirkpatrick, C. D. Gelatt Jr, M. P. Vecchi, Science **220** 671 (1983).

[2] V. Cerný, J. Optim. Theor. and Appl. **45**: 41 (1985).

[3] V. Granville, M. Krivanek, J.-P. Rasson, J.-P., IEEE Trans. on Pattern Analysis and Machine Intelligence **16** 652 (1994).

[4] A. B. Finnila, M. A. Gomez, C. Sebenik, C. Stenson and D. J. Doll, Chem. Phys. Lett. 219 343 (1994).

[5] T. Kadowaki and H. Nishimori, Phys. Rev. E 58 5355 (1998)

[6] G. E. Santoro, R. Martonak, E. Tosatti, and R. Car, Science **295**, 2427 (2002).

[7] D. Bitko, T. F. Rosenbaum, and G. Aeppli, Phys. Rev. Lett. **77**, 940 (1996).

[8] J. Brooke, D. Bitko, T. F. Rosenbaum and G. Aeppli, Science 284 779 (1999).

[9] E. Farhi, J. Goldstone, S. Gutmann, J. Lapan, A. Ludgren and D. Preda, Science **292** 472 (2001).

[10] T. Hogg, Phys. Rev. A **67**, 022314 (2003).

[11] A. Das and B. K. Chakrabarti, Rev. Mod. Phys. 80 1061 (2008).

[12] M. W. Johnson et al., Nature **473**, 194 (2011).

[13] The *D-Wave Two* quantum annealing machine manufactured by D-wave Systems; `http://www.dwavesys.com/`.

[14] S. Boixo, T. F. Rønnow, S. V. Isakov, Z. Wang, D. Wecker, D. A. Lidar, J. M. Martinis, and M. Troyer, Nature Phys. **10**, 218 (2014).

[15] J. A. Smoli and G. Smith, Frontiers in Physics **2**, 52 (2014).

[16] B. Altshuler, H. Krovi, and J. Roland, arXiv:0908.2782v2

[17] V. Bapst, L. Foini, F. Krzakala, G. Semerjian, F. Zamponi, Phys. Rep. **523**, 127 (2013).

[18] C. De Grandi, A. Polkovnikov, and A. W. Sandvik, Phys. Rev. B **84**, 224303, (2011).

[19] C.-W. Liu, A. Polkovnikov, and A. W. Sandvik, Phys. Rev. B **87**, 174302 (2013).

[20] L. Zdeborová and F. Krzakała, Phys. Rev. E **76**, 031131 (2007).

[21] F. Krzakała and L. Zdeborová, Euro. Phys. Lett. **81**, 57005, (2008).

[22] E. Farhi, D. Gosset, I. Hen, A. W. Sandvik, P. Shor, A. P. Young, and F. Zamponi, Phys. Rev. A **86**, 052334 (2012).

[23] T. Kato, J. Phys. Soc. Jpn. **5**, 435 (1951).

[24] A. Messiah, *Quantum Mechanics* (North-Holland, Amsterdam, 1962).

[25] E. Farhi, J. Goldstone, and S. Gutmann, arXiv:quant-ph/0201031.

[26] A. P. Young, S. Knysh, and V. N. Smelyanskiy, Phys. Rev. Lett. **101**, 170503 (2008).

[27] A. P. Young, S. Knysh, and V. N. Smelyanskiy, Phys. Rev. Lett. **104**, 020502 (2010).

[28] C. De Grandi, A. Polkovnikov, and A. W. Sandvik, J. Phys.: Condens. Matter **25** 404216 (2013).

[29] A. Steger and N. C. Wormald, Combinatorics, Prob. and Comput. **8**, 377 (1999).

[30] T. W. B. Kibble, J. Phys. A: Math. Gen. **9**, 1387 (1976).

[31] W. H. Zurek, Nature **317**, 505 (1985).

[32] A. Polkovnikov, Phys. Rev. B **72**, 161201(R) (2005).

[33] W. H. Zurek, U. Dorner, P. Zoller, Phys. Rev. Lett. **95**, 105701 (2005).

[34] J. Dziarmaga, Phys. Rev. Lett. **95**, 245701 (2005).

[35] J. Dziarmaga, Adv. Phys. **59**, 1063 (2010).

[36] C. De Grandi, V. Gritsev, and A. Polkovnikov, Phys. Rev. B **81**, 012303 (2010).

[37] A. Polkovnikov, K. Sengupta, A. Silva, and M. Vengalattore, Rev. Mod. Phys. **83**, 863, (2011).

[38] C.-W. Liu, A. Polkovnikov, and A. W. Sandvik, Phys. Rev. B **89**, 054307 (2014).

[39] G. E. Santoro and E. Tosatti, J. Phys. A: Math. Gen. **39** 393 (2006).

[40] H. Rieger and A. P. Young, Phys. Rev. Lett. 72, 4141 (1994).

[41] A. W. Sandvik, Phys. Rev. E **68**, 056701 (2003).

[42] C.-W. Liu, A. Polkovnikov, and A. W. Sandvik (in preparation).

[43] N. Read, S. Sachdev, and J. Ye, Phys. Rev. B **52**, 384 (1995).

[44] J. Miller and D. A. Huse, Phys. Rev. Lett. 70, 3147 (1993).

[45] P. Ray, B. K. Chakrabarti and A. Chakrabarti, Phys. Rev. B **39** 11828 (1989).

[46] J. V. Alvarez and F. Ritort, J. Phys. A: Math. Gen. **29**, 7355 (1996).

[47] H. Nishimori, J. Tsuda, S. Knysh, Phys. Rev. E **91**, 012104 (2015).

[48] C. Castelnovo, C. Chamon, C. Mudry, and P. Pujol, Ann. Phys. **318**, 316 (2005).